Crossover from a displacive to an order-disorder transition in the nonlinear-polarizability model

M. Stachiotti, A. Dobry, and R. Migoni
Instituto de Física Rosario, 27 de Febrero 210 Bis, 2000 Rosario, Argentina

A. Bussmann-Holder
Max-Planck-Institut für Festkörperforschung, 7000 Stuttgart 80, Germany
(Received 20 July 1992; revised manuscript received 5 October 1992)

The dynamics of a two-dimensional shell model with a double-well potential in the core-shell interaction is simulated by means of molecular-dynamics techniques. Snapshots of the lattice displacement pattern reveal the presence of precursor regions in the high-temperature phase, while in the low-temperature phase the dynamical structure factor exhibits a quasielastic component in addition to the ferroelectric soft-mode peak. On the other hand, the local dynamics of particles are characterized by two different time scales corresponding to the coexistence of interwell and intrawell motions. In the vicinity of the structural-phase-transition temperature a crossover from a displacive to an order-disorder transition is observed, which may explain the experimentally observed discrepancies of the nature of the phase transition.

I. INTRODUCTION

The mechanism of the ferroelectric phase transitions in oxide perovskites remains the object of many experimental investigations, e.g., infrared spectroscopy and Raman-, hyper-Raman-, and inelastic-neutron-scattering experiments, as well as electron-paramagnetic-resonance (EPR) and dielectric measurements. For the pure systems $BaTiO_3$, $PbTiO_3$, and $KNbO_3$, as well as the mixed compounds $KTa_{1-x}Nb_xO_3$ and $Sr_{1-x}Ba_xTiO_3$, contradictory results were obtained concerning the mechanisms of their structural phase transitions. A displacive mechanism driven by the instability of a soft ferroelectric mode was supported by early experiments on $BaTiO_3$ and the incipient ferroelectrics $SrTiO_3$ and $KTaO_3$.[1] An order-disorder picture was derived initially for $BaTiO_3$ from the observation of strong diffusive x-ray scattering and was later supported by the observation of Raman activity above the cubic-tetragonal transition and more detailed infrared and dielectric measurements and EPR spectroscopy.[2,3] In $BaTiO_3$ the soft-mode damping increases steadily with decreasing temperature in the paraelectric phase, surpasses the overdamping limit several hundred degrees above the transition, and becomes heavily overdamped near T_c. The soft-mode frequency obtained from infrared spectra remains finite at T_c, and a large discrepancy is observed between the capacitance dielectric constant and the one obtained from the lattice modes. An additional relaxation mechanism has to be invoked near T_c in order to explain the divergence of the experimental dielectric constant. Hyper-Raman spectra are compatible with this interpretation, although these data can also be fitted by assuming only one heavily overdamped oscillator whose frequency decreases monotonically and vanishes at T_c.[4] The observation of a central component in the Raman spectrum of $BaTiO_3$ (Ref. 5) provided direct evidence of a relaxational motion, which, by means of dielectric measurements, was found to be monodispersive and with a characteristic frequency in the 10^8-Hz range.[6] Similar phenomena are observed in $KNbO_3$,[5,7] $PbTiO_3$,[8] and $KTa_{1-x}Nb_xO_3$.[9] Relaxational dynamics were also observed in the incipient ferroelectrics $KTaO_3$ and $SrTiO_3$ at low temperatures.[10] However, in these materials, as well as in $PbTiO_3$, the ferroelectric soft mode remains underdamped and well defined.

An explanation of the experimental data can be given in terms of a crossover regime from displacive to an order-disorder transition in the vicinity of the phase-transition temperature T_c. Generally, this behavior can be found if the critical motion of the ions, which freezes out at T_c, possesses two components with different time scales. While one component is associated with quasiharmonic oscillations around the equilibrium positions and corresponds to the soft-mode frequency, the other component refers to a relaxational motion of the central transition-metal ion between two equilibrium sites. While the quasiharmonic oscillations yield a displacive mechanism, the relaxational motion introduces the order-disorder character, which simultaneously shows that the transition-metal elements: i.e., Ta, Nb, Ti, and Pb remain off center for time intervals $\leq 10^{-8}$ s, as deduced from NMR experiments.[11] The transition is characterized by a critical slowing down of correlated fluctuations as T_c is approached, independent of the magnitude of T_c.

Theoretically, the structural phase transitions of perovskite oxides can be described within a rigid-ion model with local double-well potentials and nearest-neighbor interactions only.[12] Computer-simulation techniques[13,14] as well as analytical work[15]— using this simple model—confirm the crossover behavior from displacive to an order-disorder transition. Molecular-dynamics simulations of the model reveal the appearance of a central peak in the dynamical structure factor and the for-

mation of clusters of locally ordered regions. The critical exponents obtained from the model are in agreement with the experiment, but only qualitative agreement of the characteristic temperature-dependent properties is obtained. Another obvious shortcome of this rigid-ion approach with on-site double-well potentials is the loss of translational invariance and the decoupling of the dynamics to other branches than the soft mode. This obviously severely restricts the applicability of the model to such systems. The missing information of mode coupling and interaction phenomena might explain the purely qualitative features of the model. Furthermore, electronic degrees of freedom are neglected, which play an important role in these highly polarizable compounds.

A more realistic description of the lattice dynamics of oxide perovskites could be obtained within a nonlinear shell model. The microscopic reason of this model is based on the local instability of the oxygen ion O^{2-}. This instability induces a temperature- and volume-dependent anisotropic polarizability which—lattice dynamically—is simulated by an onsite ϕ_4 potential in the electron-ion interaction, i.e., the nonlinear shell model.[16] Model calculations of phonon dispersion relations, second-order Raman spectra, temperature dependence of the soft-mode frequency, and coupled branches, as well as defect properties, are in excellent agreement with experimental data.

Calculations have been performed in particular for $KTaO_3$,[17] $SrTiO_3$,[16,18,19] $BaTiO_3$,[20] Nb:$KTaO_3$,[21] and Li:$KTaO_3$.[22,23] To avoid the use of too many parameters and to achieve an analytically treatable form of this model, a reduction of the three-dimensional model to a pseudo-one-dimensional version was considered,[24] which has been widely applied[25] and keeps all necessary dynamical information. In particular, the coupling of the soft mode to the acoustic branch[26] explains the experimentally observed anomalies in this mode when approaching the phase-transition temperature. Another highly interesting feature of the simplified nonlinear shell model is the finding of exact nonlinear solutions[27,28,29] which describe domain-wall motions and q-dependent anomalies in certain phonon modes. For the calculation of the temperature-dependent dynamic and thermodynamic properties, the three-dimensional as well as the one-dimensional model made use of the self-consistent phonon approximation (SPA).[26,30] This corresponds to a temperature-dependent linearization of the nonlinear potential and a replacement of the higher-order interactions by effective temperature-dependent quantities, to be determined self-consistently. For a purely displacive-type phase transition, this mean-field theory has been shown to be valid, but it obviously fails in the order-disorder limit. Thus important features as observed in, e.g., $BaTiO_3$ cannot be explained within the SPA and especially the crossover from displacive to an order-disorder transition lies beyond this approximation.

The aim of the present work is to avoid the above-mentioned shortcoming of the SPA by analyzing the nonlinear shell model with molecular-dynamics (MD) techniques. This method allows one to treat the nonlinear potential without linearization schemes and reveals realistically the dynamics of the ions in the vicinity of T_c. The pseudo-one-dimensional model is extended to two dimensions in order to obtain finite transition temperatures, which in the one-dimensional case were obtained by isotropic spherical three-dimensional integration techniques.

II. MODEL AND COMPUTATIONAL DETAILS

The model we use is depicted in Fig. 1. It represents an extension of the pseudo-one-dimensional model, but using all conventions inferred in that version: i.e., M_1 refers to the mass of the polarizable cluster BO_3 of perovskites ABO_3 and M_2 to the cationic A sublattice. f and f' are nearest-neighbor core-shell and core-core force constants. The instability of the ferroelectric soft mode is attributed to attractive Coulomb forces which are included in the harmonic core-shell coupling g_2. Consequently, g_2 represents an attractive interaction. Stabilization of the soft-mode frequency in the paraelectric and ferroelectric phases is achieved via the repulsive fourth-order core-shell coupling g_4. The equations of motion read, using the adiabatic condition for the shell masses,

$$M_1 \ddot{u}_{1\alpha}^{m,n} = f'(u_{1\alpha}^{m+1,n} + u_{1\alpha}^{m-1,n} + u_{1\alpha}^{m,n+1} + u_{1\alpha}^{m,n-1} - 4u_{1\alpha}^{m,n}) + g_2 w_\alpha^{m,n} + g_4 (w_\alpha^{m,n})^3 , \quad (1)$$

$$M_2 \ddot{u}_{2\alpha}^{m,n} = 2f(u_{1\alpha}^{m,n} + u_{1\alpha}^{m+1,n-1} + u_{1\alpha}^{m,n-1} + u_{1\alpha}^{m+1n,} + w_\alpha^{m,n} + w_\alpha^{m+1,n-1} + w_\alpha^{m,n-1} + w_\alpha^{m+1,n} - 4u_{2\alpha}^{m,n}) , \quad (2)$$

$$0 = 2f(u_{2\alpha}^{m,n} + u_{2\alpha}^{m-1,n+1} + u_{2\alpha}^{m,n+1} + u_{2\alpha}^{m-1,n} - 4w_\alpha^{m,n} - 4u_{1\alpha}^{m,n}) - g_2 w_\alpha^{m,n} - g_4 (w_\alpha^{m,n})^3 , \quad (3)$$

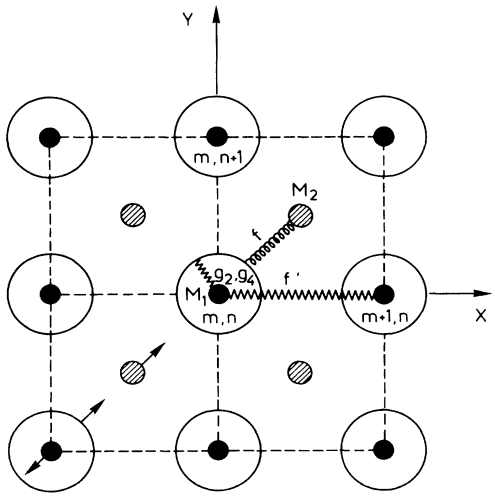

FIG. 1. Two-dimensional diatomic nonlinear polarizability model. The arrows on shells and cores in the left bottom corner of the figure indicate their respective displacements in the ferroelectric phase.

where $u_{i\alpha}^{m,n}$ is the core displacement component α ($\alpha=x,y$) of ion i ($i=1,2$) in the cell (m,n) and M_i are the ionic masses.

It is important to note here that $w_\alpha^{m,n}$ is the relative core-shell displacement coordinate, i.e., $w_\alpha^{m,n}=v_\alpha^{m,n}-u_\alpha^{m,n}$ with $v_\alpha^{m,n}$ being the shell displacement, as the use of this relative displacement coordinate contributes significantly to the renormalization of the soft-mode frequency and induces substantial differences as compared to the rigid-ion anharmonic lattice model.

The SPA corresponds to a first-cumulant expansion of the cubic terms in w_α^{mn} and introduces an effective temperature-dependent pseudoharmonic coupling:

$$g(T)=g_2+3g_4\langle w_\alpha^2\rangle , \tag{4}$$

where $\langle w_\alpha^2\rangle$ is the self-consistent thermal average of the relative displacement squared at temperature T. The temperature dependence of the transverse-optic-mode frequency at $q=0$, i.e., the ferroelectric soft-mode frequency, is given by

$$\omega_F^2(q=0)=\left[\frac{1}{M_1}+\frac{1}{M_2}\right]\frac{8fg(T)}{8f+g(T)} . \tag{5}$$

In the displacive limit, the transition occurs for $\omega_F=0$, the critical temperature being given by the condition $g(T_c)=0$. Here it should be emphasized that an important temperature-dependent renormalization of ω_F^2 is obtained through $g(T)$ in the denominator in Eq. (5). In the limit $g(T)\approx 0$ (i.e., close to T_c), Eq. (5) reduces to the results obtained from the anharmonic rigid-ion model, valid at all temperatures T in that model. For $g(T)\gg 0$, i.e., far away from the transition point, Eq. (5) approaches the rigid-ion limit, and consequently $\omega_F^2(q=0)$ saturates. This regime is not obtained in the anharmonic rigid-ion model, but agrees quantitatively with experimental data.

As already mentioned above, MD techniques treat anharmonicities without approximations. In the following we employ a constant-temperature MD procedure to investigate the lattice dynamics in the neighborhood of the structural transition. In order to obtain reasonable temperature control and simultaneously maintain stability, we employ a predictor-corrector algorithm.[31] This algorithm includes the velocities in the predictor used to calculate the positions such that the system's temperature may be adjusted by rescaling the particles velocities after each time step. Introducing the dimensionless quantities

$$M=\frac{M_1}{M_2} , \quad F=\frac{2f}{|g_2|} , \quad F'=\frac{f'}{|g_2|} , \quad w_0=\left[\frac{|g_2|}{g_4}\right]^{1/2} ,$$

$$U_{1\alpha}^{m,n}=\frac{u_{1\alpha}^{m,n}}{w_0} , \quad U_{2\alpha}^{m,n}=\frac{u_{2\alpha}^{m,n}}{w_0} ,$$

$$W_\alpha^{m,n}=\frac{w_\alpha^{m,n}}{w_0} , \quad \tilde{t}=\left[\frac{|g_2|}{M_2}\right]^{1/2} t .$$

The equations of motion are rewritten as

$$M\ddot{U}_{1\alpha}^{m,n}=F'(U_{1\alpha}^{m+1,n}+U_{1\alpha}^{m-1,n}+U_{1\alpha}^{m,n+1}+U_{1\alpha}^{m,n-1}-4U_{1\alpha}^{m,n})-W_\alpha^{m,n}+(W_\alpha^{m,n})^3 , \tag{6}$$

$$\ddot{U}_{2\alpha}^{m,n}=F(U_{1\alpha}^{m,n}+U_{1\alpha}^{m+1,n-1}+U_{1\alpha}^{m,n-1}+U_{1\alpha}^{m+1,n}+W_\alpha^{m,n}+W_\alpha^{m+1,n-1}+W_\alpha^{m,n-1}+W_\alpha^{m+1,n}-4U_{2\alpha}^{m,n}) , \tag{7}$$

$$0=F(U_{2\alpha}^{m,n}+U_{2\alpha}^{m-1,n+1}+U_{2\alpha}^{m,n+1}+U_{2\alpha}^{m-1,n}-4U_{1\alpha}^{m,n})+(1-4F)W_\alpha^{m,n}-(W_\alpha^{m,n})^3 . \tag{8}$$

Equation (8), which is cubic in the relative core-shell displacement coordinate, can be solved for $u_{1\alpha}^{m,n}, u_{2\alpha}^{m,n}$ and yields a complex nonlinear potential in the core coordinates. The solutions which are obtained within each iterative step of the MD calculation are subsequently inserted in Eqs. (6) and (7).

III. RESULTS AND DISCUSSION

The MD simulation is performed for a square lattice of 32×32 unit cells with periodic boundary conditions. The values of the dimensionless coupling constants are $F=2$, $F'=0.7$, and $M=4$. The runs were performed for 2^{14} steps after zero time, using step size of $\Delta\tilde{t}=0.1$. The temperature is defined by $\tilde{T}=(g_4/g_2)k_BT$ and has been calculated as the mean kinetic energy of the particles.

In order to identify the phase transition, the following vectorial order parameter is introduced:

$$Q_j=N^{-1/2}\langle Q(q=0,j)\rangle=\langle M^{1/2}U_1-U_2\rangle , \tag{9}$$

where $Q(q=0,j)$ is the amplitude of the soft-mode normal coordinate and describes the ionic displacements in the distorted phase. A nonzero value of this order parameter indicates the presence of the ferroelectric phase. For the above set of parameters, we obtain $\tilde{T}_c=0.54$.

We calculate the leading approximation to the dynamical structure factor as the space-time Fourier transform of the core-core displacement correlation function. The results for $S(q=0,\omega)$ at various temperatures above $\tilde{T}_c$ are illustrated in Fig. 2. At high temperatures [Fig. 2(a)], a phonon peak which corresponds to the ferroelectric soft mode is well resolved and the SPA value (indicated by an arrow) is in reasonable agreement with the position of this peak. Here the SPA value is not obtained by means of Eqs. (4) and (5), but by inserting the value of w_α^2, evaluated in the MD procedure in Eq. (4).

With decreasing temperature the ferroelectric phonon peak softens and a broad central component appears at $\tilde{T}>\tilde{T}_c$ [Fig. 2(b)]. The structure below ~ 135 frequency units should be viewed as a single very broad peak. On approaching $\tilde{T}_c$ further, the central peak becomes narrower and more intense. On the other hand, the soft-phonon resonance intensity decreases and disappears many degrees above the transition [Figs. 2(c) and 2(d)]. We examined with a large intensity scale the tail of the central peak in Figs. 2(c) and 2(d) and could not observe anything corresponding to the soft-phonon peak which

may be already highly overdamped.

Note that the SPA value of the soft mode stays at 130 frequency units below $\tilde{T}=1.4\tilde{T}_c$, while, for reference, the zone-boundary acoustic-mode frequency has a value of 118 frequency units.

The microscopic origin of the central peak in systems with structural phase transition is still not known.[32] However, a possible explanation could be the appearance of precursor effects. The slow motion of the domain walls could be the origin for this quasistatic component in the spectrum of the system. In fact a MD simulation of a one-component displacement model shows that the central peak is related to traveling cluster waves.[14] To elucidate this point in more detail, we have analyzed the possible formation of precursor clusters, suggesting that also in the present model the ferroelectric phase transition is of order-disorder type.

In the investigated two-dimensional model, the order parameter has two independent components due to the soft-mode degeneracy. In fact, there are four different cluster patterns related to four ferroelectric domains which can be generated by the spatial direction of the local order parameter. The existence of correlated fluctuations in the cubic phase implies that in small clusters of the lattice the local order parameter has one of the possible four orientations which would lead to small locally ordered phases. In the ferroelectric phase, the system is in one of the four possible spatial orientations and all the cells are polarized in the same direction. Therefore, in order to investigate the formation of precursor clusters above the transition, snapshots of instantaneous configurations are shown for various temperatures in Fig. 3. Four symbols distinguish the four different possible orientations of cell polarizations. For $\tilde{T}\gg\tilde{T}_c$ [Fig. 3(a)], fully uncorrelated polarizations are seen, while well below $\tilde{T}_c$ [Fig. 3(d)] the whole system has the same polarization except for isolated cell fluctuations. At temperatures close above [Fig. 3(b)] and below [Fig. 3(c)] $\tilde{T}_c$ clusters of coherent polarization are clearly distinguished. The dynamics of these regions give rise to the central peak observed in Fig. 2.

Another interesting question is related to the local dynamics of the particles, since this determines the lifetime of the correlated fluctuations. As already pointed out, several experiments provide evidence of noncubic local symmetry in the paraelectric phase of oxide perovskites.[2,3,11] From dielectric measurements a lifetime of 10^{-8}–10^{-9} s can be deduced for off-center posi-

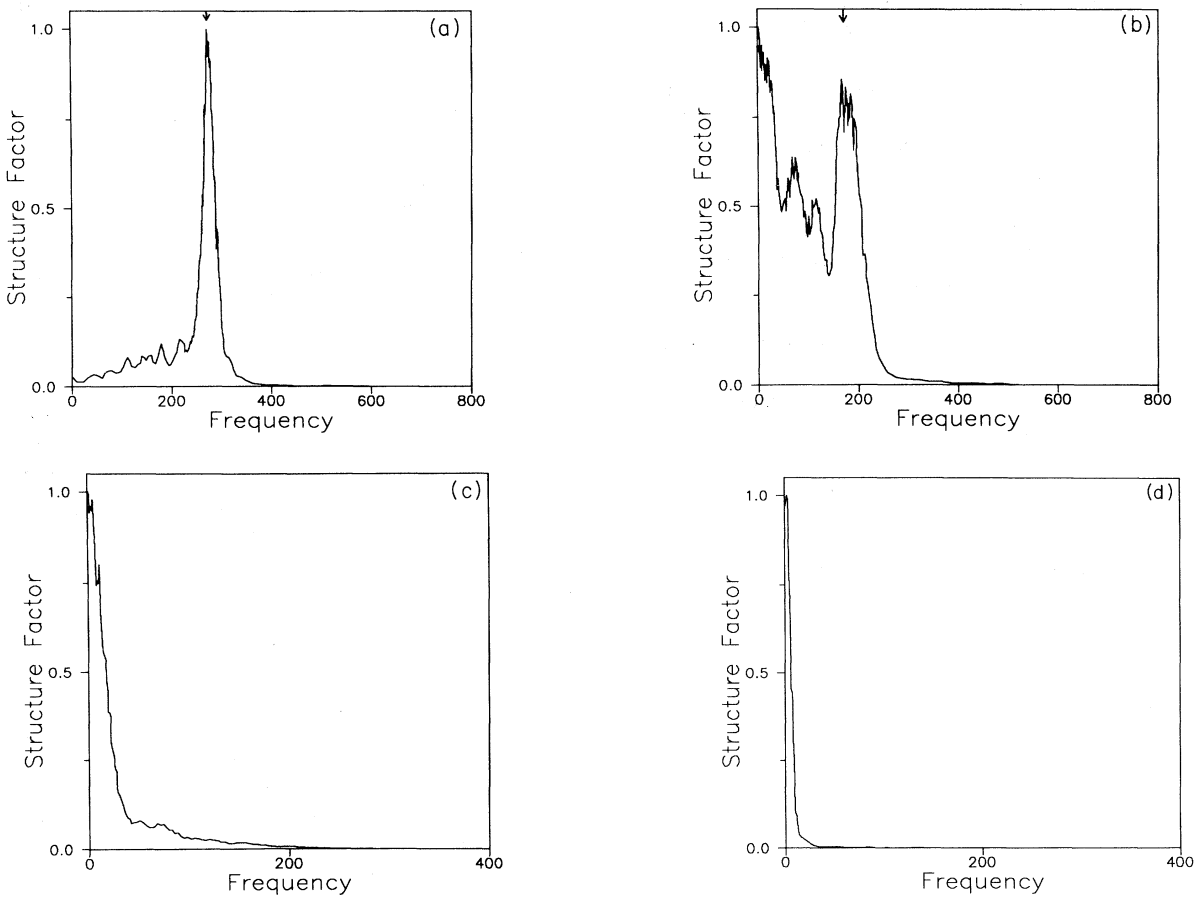

FIG. 2. Dynamical structure factor $S(q=0,\omega)$ in the paraelectric phase for several values of $\tilde{T}/\tilde{T}_c$: (a) 11.4, (b) 2.9, (c) 1.4, and (d) 1.04. The arrow indicates the SPA value of the ferroelectric mode in each case. Frequencies are given in dimensionless units. The intensity scale sets the absolute maximum equal to 1.

tions.[6,10] In order to investigate whether a similar situation appears in our model, we follow the movement of the particles in a given arbitrary unit cell. In Fig. 4 the time evolution for the shell and core coordinates is shown at different temperatures. At high temperatures the shell and cores show oscillatory dynamics around their perfect lattice sites [Fig. 4(a)]. Simultaneously, the structure factor shows the soft-mode phonon peak only [Fig. 2(a)]. Close to T_c [Fig. 4(b)], a coexistence of interwell and intrawell motion appears on two different time scales. The shell and cores remain in a given off-center position and jump to the other equivalent site after ~ 1000 MD steps [Fig. 4(b)]. They also show oscillatory dynamics around these off-center positions. Obviously, there is a clear relation between the local interwell motion and the appearance of precursor clusters, which points to the relevant mechanism for the existence of the central peak in our model.

IV. SUMMARY AND CONCLUSIONS

We have shown that the two-dimensional version of the nonlinear polarizability model for ferroelectric soft modes accounts for the experimentally observed crossover from the displacive soft-mode picture to order-disorder dynamics near the transition. The results of our MD simulations are in agreement with experiments, especially in the vicinity of $\tilde{T}_c$. This refers in particular to the coexistence of oscillatory and relaxational motions on different time scales. Each particle performs a rapid phononlike motion around its momentary off-center position and changes its position to the other equivalent position after much longer times. The instantaneous displacement patterns show clusters of particles of coherent polarization. Within each correlated region, the particles oscillate around a given local ferroelectric configuration. Consequently, a low-frequency peak in the dynamic response appears because of the slow dynamics of the ordered precursor regions. The central peak intensity is found to increase while its width decreases as $\tilde{T}_c$ is approached. This behavior is related to a growth of the cluster lifetime as the central peak half-width is proportional to the inverse lifetime while its height is proportional to it. Finally, the soft-phonon peak disappears from the dynamic response well above $\tilde{T}_c$, thus indicating that the ferroelectric mode becomes heavily overdamped.

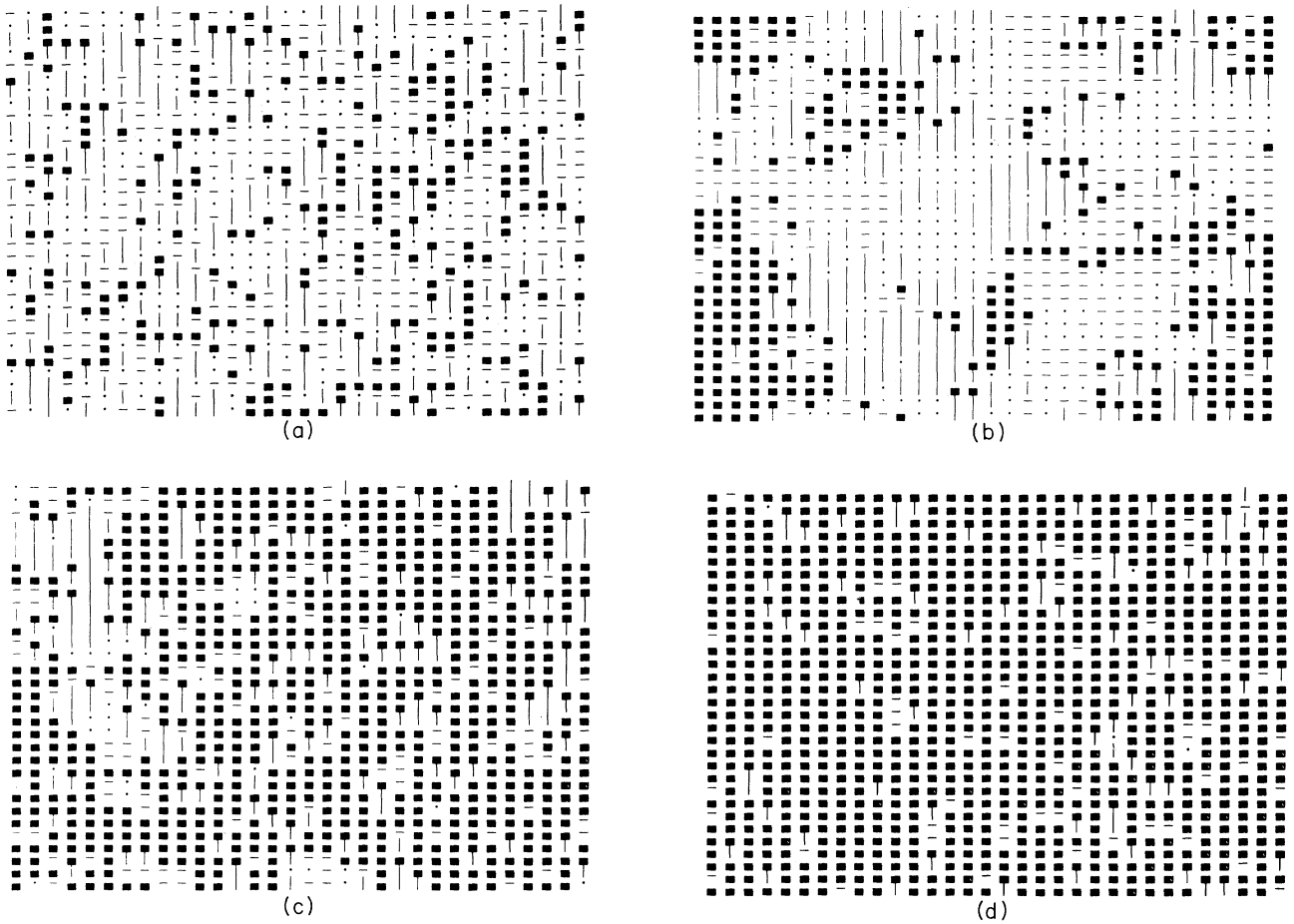

FIG. 3. Instantaneous cell polarization patterns in the paraelectric [(a) and (b)] and ferroelectric [(c) and (d)] phase for several values of $\tilde{T}/\tilde{T}_c$: (a) 11.4, (b) 1.15, (c) 0.94, and (d) 0.66. The symbols □, ·, |, and − refer to the four different polarization domains, discussed in the text.

The SPA frequency of this mode is found to saturate and remain finite at $\tilde{T}_c$.

The results obtained from MD techniques clearly indicate that an order-disorder mechanism drives the structural instability in the vicinity of T_c, while former SPA results favor a displacive-type picture. As both methods are complementary, it can be concluded that, for temperatures larger than T_c, displacive-type behavior should be observed, while close to T_c critical fluctuations have to be taken into account seriously; i.e., the SPA is

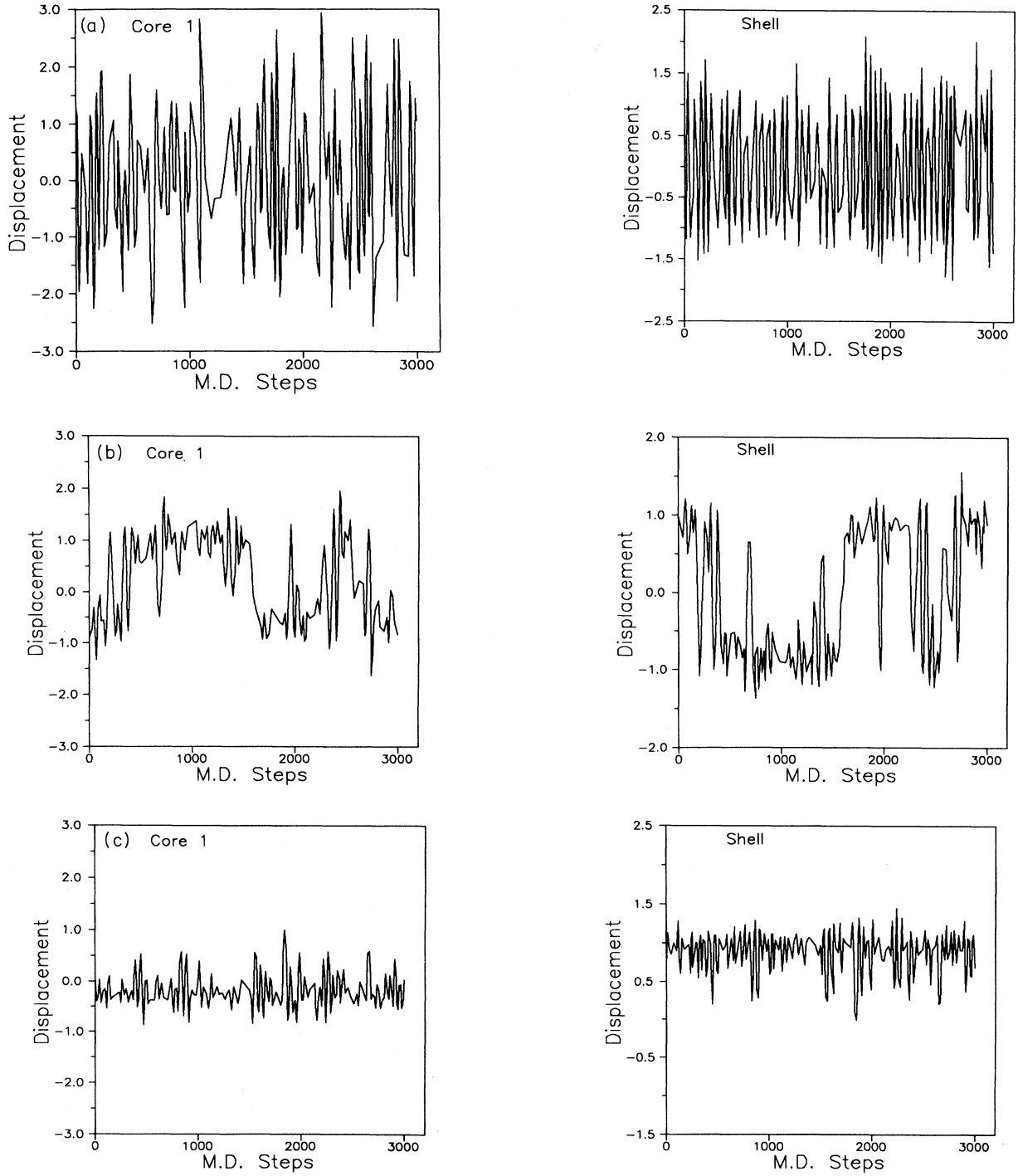

FIG. 4. Time evolution of the core and shell displacement in the direction (1,1) at a given site 1 for different values of $\tilde{T}/\tilde{T}_c$: (a) 11.4, (b) 1.15, and (c) 0.85. Note in (c) that the finite mean displacements of cores and shells are observed in the ferroelectric phase. Similar results are obtained for the second core 2.

no longer valid in this regime, and order-disorder-type features are consequently observed. Thus the complementary character of MD and SPA fully accounts for the partially conflicting results obtained in various experiments.

Finally, it should be mentioned that the three-dimensional polarizability model fully accounts for realistic ion polarizabilities and short-range and Coulomb interactions. As the ferroelectric soft-mode instability results from a compensation of short-range and Coulomb forces, all short-range forces are repulsive here.[16,17,20,21] Stabilization of the lattice is achieved via the anisotropic fourth-order core-shell interaction, which induces an effective double-well potential in the ferroelectric normal-mode coordinate. Thus it is to be expected that the qualitative features obtained from the reduced model described above will also be recovered in three dimensions, and quantitative aspects for order-disorder dynamics for specific ferroelectrics can be obtained especially in the vicinity of T_c.

ACKNOWLEDGMENTS

M.S. and R.M. acknowledge support from the Consejo Nacional de Investigaciones Científicas y Técnicas, and A.D. acknowledge support from the Consejo de Investigaciones de la UNR.

[1]M. E. Lines and A. M. Glass, *Principles and Applications of Ferroelectrics and Related Materials* (Clarendon, Oxford, 1977).

[2]K. A. Müller, Y. Luspin, J. L. Servoin, and F. Gervais, J. Phys. (Paris) Lett. **43**, L-537 (1982), and references therein.

[3]K. A. Müller and W. Berlinger, Phys. Rev. B **34**, 6130 (1986).

[4]H. Vogt, J. Sanjurjo, and G. Rossbroich, Phys. Rev. B **26**, 5904 (1982); H. Presting, J. Sanjurjo, and H. Vogt, *ibid.* **28**, 5904 (1983).

[5]J. P. Sokoloff, L. L. Chase, and D. Rytz, Phys. Rev. B **38**, 597 (1988).

[6]M. Maglione, R. Böhmer, A. Loidl, and U. Höchli, Phys. Rev. B **40**, 11 441 (1989).

[7]M. D. Fontana, G. Métrat, J. Servoin, and F. Gervais, J. Phys. C **16**, 483 (1984), and references therein.

[8]M. D. Fontana, H. Idrissi, G. E. Kugel, and K. Wojcik, J. Phys. Condens. Matter **3**, 8695 (1991).

[9]M. D. Fontana, E. Bouziane, and G. Kugel, J. Phys. Condens. Matter **2**, 8681 (1990), and references therein.

[10]M. Maglione, S. Rod, and U. T. Höchli, Europhys. Lett. **4**, 631 (1987).

[11]S. Rod, F. Borsa, and J. J. van der Klink, Phys. Rev. B **38**, 2267 (1988).

[12]A. D. Bruce, Adv. Phys. **29**, 111 (1980).

[13]T. Schneider and E. Stoll, Phys. Rev. B **17**, 1302 (1978).

[14]T. Schneider and E. Stoll, Phys. Rev. B **13**, 1216 (1975).

[15]J. A. Krumhansl and J. R. Schrieffer, Phys. Rev. B **11**, 3535 (1975).

[16]R. Migoni, H. Bilz, and D. Bäuerle, Phys. Rev. Lett. **37**, 1155 (1976).

[17]C. Perry, R. Currat, H. Buhay, R. Migoni, W. Stirling, and J. Axe, Phys. Rev. B **39**, 8666 (1989).

[18]R. L. Migoni, K. H. Rieder, K. Fisher, and H. Bilz, Ferroelectrics **13**, 377 (1976).

[19]R. L. Migoni, thesis, Stuttgart University, 1976.

[20]D. Khatib, R. L. Migoni, G. E. Kugel, and L. Godefroy, J. Phys. Condens. Matter **1**, 9811 (1991).

[21]G. E. Kugel, M. D. Fontana, and W. Kress, Phys. Rev. B **35**, 813 (1987).

[22]M. Stachiotti and R. Migoni, J. Phys. Condens. Matter **2**, 4341 (1990).

[23]M. Stachiotti, R. Migoni, and U. Höchli, J. Phys. Condens. Matter **3**, 3689 (1991).

[24]H. Bilz. A. Bussmann, G. Benedek, H. Büttner, and D. Strauch, Ferroelectrics **25**, 339 (1980).

[25]A. Bussmann-Holder, H. Bilz, and G. Benedek, Phys. Rev. B **39**, 9214 (1989).

[26]H. Bilz, G. Benedek, and A. Bussmann-Holder, Phys. Rev. B **35**, 4840 (1987).

[27]G. Benedek, A. Bussmann-Holder, and H. Bilz, Phys. Rev. B **36**, 630 (1987).

[28]H. Bilz, H. Büttner, A. Bussmann-Holder, W. Kress, and U. Schröder, Phys. Rev. Lett. **48**, 264 (1982).

[29]A. Dobry, R. Migoni, and H. A. Ceccatto, Phys. Rev. B **38**, 2801 (1988).

[30]A. Dobry, A. Greco, and M. Stachiotti, Phys. Rev. B **43**, 11 166 (1991).

[31]D. Beeman, J. Comput. Phys. **20**, 130 (1976).

[32]F. Schwabl and U. C. Täuber, Phys. Rev. B **43**, 11 112 (1991).